Towards a Comprehensive Geometric Model of the Heart

Cristian Lorenz and Jens von Berg

Philips Research Laboratories Hamburg,
Röntgenstrasse 24-26, 22335 Hamburg, Germany
Cristian.Lorenz@Philips.com

Abstract. Domain knowledge about the geometrical properties of cardiac structures is an important ingredient for the segmentation of those structures in medical images or for the simulation of cardiac physiology. So far, a strong focus was put on the left ventricle due to its importance for the general pumping performance of the heart and related functional indices. However, other cardiac structures are of similar importance, e.g. the coronary arteries with respect to diagnosis and treatment of arteriosclerosis or the left atrium with respect to the treatment of atrial fibrillation. In this paper we describe the generation of a comprehensive geometric cardiac model including the four cardiac chambers and the trunks of the connected vasculature, as well as the coronary arteries and a set of cardiac landmarks. A mean geometric model has been built. A general process to add inter-individual and temporal variability is proposed and will be added in a second stage.

1 Introduction

The use of cardiac domain knowledge in terms of geometrical models of the heart has been reported in many articles (see [1] for a review). The main focus so far, was on the left ventricle and the related cardiac function and wall motion analysis. Recently, motion analysis has also been performed on the right ventricle [2] and atrium [18] and modeling approaches started to include both ventricles [3-8] or even all 4 cardiac chambers [9,17]. Other publications deal with the geometrical properties of the coronary arteries [10-12]. In clinical practice, two trends are currently gaining importance. First of all there is a strong trend towards automation. Limited budgets in terms of money and time call for "zero-click" procedures for cardiac analysis such as functional values or coronary artery assessment. A comprehensive image based cardiac diagnosis session, revealing all important parameters and producing all relevant image renderings needs to be finished in about 10 to 15 min. The second trend is about accomplishing a synoptic representation of the cardiac aspects of the patient: How is the stenosed coronary artery related to the damaged myocardial tissue? Does the wall motion artifact support the myocardial perfusion findings? A key issue arising from both trends is the extensive use of cardiac domain knowledge i.e. the use of cardiac models. A third trend actually comes from the scientific desire

A.F. Frangi et al. (Eds.): FIMH 2005, LNCS 3504, pp. 102 – 112, 2005.

to understand and simulate the heart from first principles. Here, in the end, we need to include all relevant structures and the related properties into one model: The coronary arteries supplying the myocardium with oxygen, the myocardium contracting and performing a pump-action, the resulting blood flow in turn supplies oxygenated blood to the coronary arteries. Each of the three trends benefits from or even requires a comprehensive representation of all important cardiac structures in one model. In this paper the generation of such a comprehensive geometric heart model is described.

In addition to the information about shape and appearance of the object itself (as e.g. used in a model based segmentation approach), the model can provide information for proper initialization of position and pose of the object, e.g. by use of geometrical relations between the object of interest and other cardiac structures. For example the position of either manually marked or automatically detected landmarks can be used to estimate an initial spatial transformation to place the cardiac model into the image space. The landmarks used for the procedure must be part of the comprehensive model but they need not be part of the object of interest. Another possibility is a sequence of segmentation or adaptation procedures, each one being initialized with the result of the previous one. The result of an adaptation of a surface model to the left ventricle of the heart can be used to initialize the segmentation of the coronary arteries by transforming the coronary artery model into the image space and thereby restricting the search space for the subsequent coronary artery segmentation.

2 A Multi-component Model

The generation of a multi-component model raises several issues:

- **The combination of geometrical information form several sources**
  In our case, the mean geometrical model for the coronary arteries was taken from the literature [13,14], the cardiac surfaces and cardiac landmarks originate from multi-slice CT data which provides high resolution data of the complete heart (but with limited temporal resolution) and we intend to improve the motion model using cardiac MRI data which provides a better temporal but anisotropic spatial resolution and covers usually only the left and right ventricles. The information from all these sources needs to be combined.
- **The representation of consistent variability, avoiding conflicting deformation of the individual structures**
  The geometrical information provided by a comprehensive multi-object model may contain geometric entities of different representation. Some surfaces are perhaps represented as triangular meshes, others as spline surface patches, others may be represented using implicit functions. In addition to the surfaces, there may be vessel representations using centerlines and radius values etc. In this case, where we have different geometric parameterizations, the standard Eigen-value decomposition of the covariance matrix of the shape samples [15] cannot be used any longer. In addition, the available geometry samples may contain different sub-sets of the object set contained in the projected model. We think that this aspect calls for a distinct representation of the shape geometries and their variability. More specifically we propose to generate a mean comprehensive geometry model and separate deformation models, dealing with

inter-individual deformation and temporal deformation and defining each full-space deformations.

- **The representation of the topological, geometrical, anatomical, and physiological relations between sub-structures**
  For higher levels of reasoning and user interaction, a complex anatomical model needs to be augmented with information beyond pure geometry. Anatomical nomenclature and its associated relations and hierarchies will e.g. help to display processing results adequately to the clinical user or to request user input, or to inhibit penetration or intersection of certain structures by other structures, during model adaptation.

3 General Structure of the Model

The model includes a definition of a set of cardiac landmarks and their mean locations, the mean geometry of the coronary arteries (centerlines and radii), the mean surfaces of the four cardiac chambers, and the connected vascular trunks, i.e. trunks of the vena cava, the pulmonary arteries, the pulmonary veins and the aorta. The mean geometries correspond to the end-diastolic cardiac phase. In addition to the mean geometries the model will be extended to include typical deformation patterns for inter-individual deformation and for temporal deformation. The deformation patterns are expressed as smooth full space transformations, independent of the geometric structures. All geometric entities feature an anatomical label. A nomenclature table allows the lookup of the respective anatomical name of the structure. Relation tables provide information about the relation of anatomical items. Currently the relations "is-part-of", "is-child-of", and "is-connected-to" are covered. To facilitate user interaction pictograms can be added to the model. Currently a pictogram of the coronary arteries derived from the one proposed by the American Heart Association (AHA) [16] is provided. The model is intended to support mainly image processing applications. In order to do so, the pure information (e.g. geometries, variability, meta-information) covered by the model is associated with application independent model related functionality. It covers basic individualization functionality (e.g. landmark based model deformation or model to image registration), meta-information related functionality (e.g. retrieve a list of related structures for a given structure of interest), and basic user interaction (e.g. rendering of image data together with geometric entities or pictogram based user-input). The model related functionality has been implemented in Java, model persistence is achieved by serialization of the model object entities to XML files.

4 Model Generation

4.1 The Coronary Artery Model

As the basis for the coronary artery model we used measurements from J. T. Dodge et al. about the location [13] and diameters [14] of human coronary arteries as reconstructed from bi-planar angiograms. In addition to the publicized values, J. T. Dodge kindly made available an updated and enlarged list of values. Dodge

distinguishes 32 coronary artery segments. Each segment is trisected in a proximal, mid, and distal section and the center-point of each section is measured, giving in total 96 points defining the coronary artery tree. Basis for the measurements are 37 patients, categorized into three coronary supply types: right dominant, balanced and left dominant. The original point data is given in a spherical coordinate system. Based on this data, we constructed a coronary artery tree model. Since the point set provided by Dodge does not include the start and end point of each segment, we recovered the branching points by linear extrapolation and intersection with the parent segments. An interesting result of the measurements performed by Dodge, is the consistency of coronary artery location across the three supply types. The main property that differs depending on the supply type, is the tree topology, i.e. the connectivity between coronary artery segments. As a result, the arteries at the lower "back-side" of the heart are sometimes fed by right coronary artery and sometimes by the left circumflex coronary artery, but they stay mainly in place. Figure 1 shows a rendering of the resulting coronary artery model and the corresponding pictogram derived from the one recommended by the AHA [16]. The model was evaluated on multi-slice CT angiography (MSCTA) images [12]. The evaluation was restricted to the three main coronary arteries (left anterior descending, circumflex, and right coronary artery) being manually drawn in the images. The smaller branches could not be imaged with the necessary constant visibility over patient samples and were therefore left out. It could be shown that using an affine adaptation scheme, a mean residual distance between adapted model and sample lines of 2.7 mm could be achieved [12].

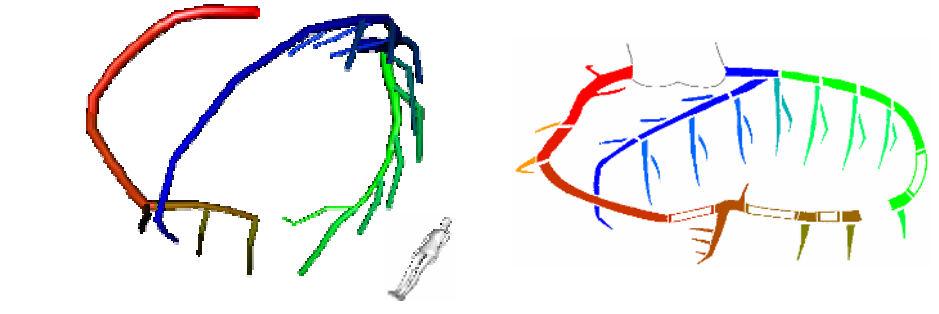

Fig. 1. Left: Coronary artery model, derived from the Measurements of Dodge et al. [13,14]. Right: Pictogram adopted from the AHA recommendation [16] using a coherent color scheme. The whitish colored coronary artery segments of the pictogram depict the variable portion depending on the supply type

4.2 Adding Landmarks to the Model

Cardiac landmarks are usually not of direct interest in cardiac diagnosis or treatment planning. However, they can serve as reference points that can be used to register image-data to image-data or model to image-data. Landmark positions may originate from user input or from automated detection algorithms. We defined a set of 25 landmarks (see figure 2). The landmarks were manually defined in 20 end-diastolic

cardiac CTA datasets in order to create a mean landmark model. In addition to the landmarks, the three main coronary arteries were defined in the CTA datasets, in order to allow a registration between landmark model and coronary artery model. In order to calculate mean landmark positions, the landmark sets need to be transformed into a common reference coordinate system. We performed a Procrustes analysis [15] to find the optimal transformations for all shape samples given the allowed transformation class (similarity transformation). In order to transform the mean landmark model into the coordinate system of the coronary artery model, the transformations resulting from the Procrustes analysis are applied to the manually delineated coronary artery centerlines of the samples. By a subsequent match of the resulting bunch of coronary arteries to the coronary artery model, and applying the resulting transformation to the landmark model, we achieve a combined coronary artery and landmark model (Fig. 2).

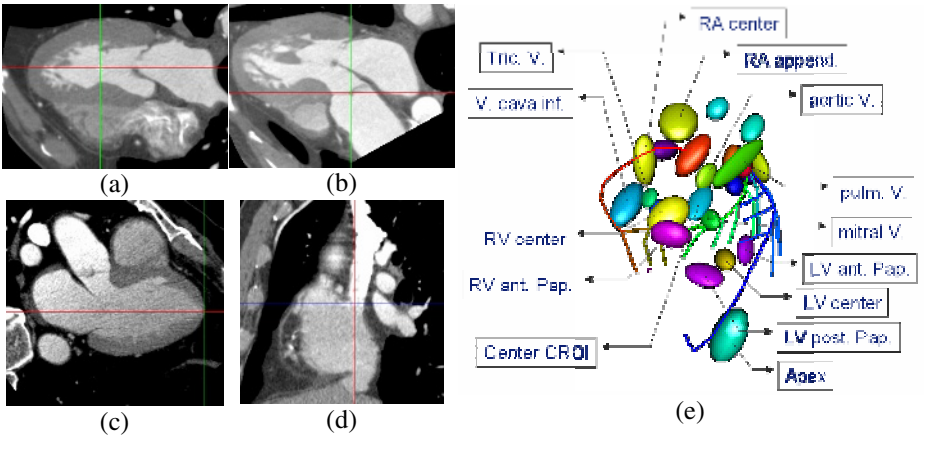

Fig. 2. Cardiac landmarks. The landmark set includes the overall center of the heart, the center-points of the four cardiac chambers, the four valve centers, apex, center of left anterior, left posterior, and right anterior papillary muscle, center points of left and right atrial appendage, left and right coronary ostium, bifurcation point of left anterior descending and circumflex coronary artery, the four ostia of the pulmonary veins, ostia of vena cava superior and inferior, and the ostium of the coronary sinus

Figures a-d: Some landmark examples, (a) center left ventricle, (b) aortic valve, (c) apex, (d) onset of vena cava superior. Figure (e) shows the error ellipsoids (directional std. deviation) centered at the landmark positions with the registered coronary artery model

4.3 Adding Cardiac Surfaces to the Model

With cardiac surfaces we mean the endo- and epicardium of the cardiac chambers and the walls of the connected vascular trunks. On the basis of state of the art 3D image material such as CT or MRI images, endo- and epicardium can often only be distinguised for the left ventricle. Therefore, for the time being, the right ventricle and the left and right atria are modeled with one surface each, representing endo- *and*

epicardium. The following structures are included in the model: Left and right ventricle, left and right atrium, trunks of vena cava superior, vena cava inferior, pulmonary artery, pulmonary veins, and aorta. The surfaces are represented as a set of connected triangular meshes. A labeling scheme allows identifying for each triangle the corresponding cardiac structure.

The standard procedure to generate an anatomical surface model starts with the (usually interactive) segmentation and labeling of a learning set of data. In a second step either a mean label image is generated [3] and subsequently triangulated, or one label image is triangulated and the resulting mesh is adapted to the other label images [19]. For the generation of our cardiac surface model we tried to circumvent the necessity of a set of segmented datasets and chose for a bootstrap method working directly on un-processed 3D images. The main reason for this choice is to avoid the extremely time consuming procedure of manual or semi-automated segmentation of all the required cardiac structures. Our method makes use of available mesh generation and manipulation functionality [20] as well as active surface adaptation procedures for 3D image segmentation [21]. The procedure is somewhat similar to the one described in [19], but circumvents the use of labeled images. It consists of four main steps:

1. All cardiac structures of interest are independently interactively segmented in one high-quality, "normal" CTA image (root image). The segmentation is performed using an active shape procedure [21] starting from a simple, e.g. ellipsoidal or tubular shape. The segmentation of the individual structures is iteratively improved until a sufficient segmentation quality is reached. Each iteration consists of an automatic active surface based surface to image adaptation and a subsequent interactive correction at locations of insufficient match. The interactive corrections are mesh deformation operations working on an adjustable influence range [20]. The result of this step is a set of closed surfaces, each resembling one cardiac structure, i.e. one for the left ventricle, one for the left atrium etc.
2. Next, the set of surfaces from part one are merged to create one connected and labeled surface mesh. It requires the successive application of a handful of basic operations on surface meshes such as volumetric operations (union or difference operation applied to two closed surfaces), intersection and cut operations, and mesh refinement operations (e.g. in order to remove small triangles or to change the resolution of the triangulation) [22]. As long as the structures that need to be merged are overlapping, the merging operation can be performed automatically, given a set of closed surfaces and the desired triangle size. In case of non-overlapping structures that still need to be connected, some handcrafting is required. The result of this step is one connected and labeled mesh covering all input structures. The mesh resembles the shape of the structures as given in the input image.
3. Then, the mesh resulting from part two is adapted to a learning set of images. For initialization, a similarity transformation is applied to the vertices of the mesh resulting from part two. The transformation is estimated [23] on the basis of a set of cardiac landmarks defined in the root image and the image under

consideration. After initialization the mesh is semi-automatically adapted to the image similarly to the procedure in part two. The active surface method used during the adaptation procedure contains a shape term that minimizes triangle edge ratio differences between the model shape and the adapted shape. This leads to a predominant conservation of point correspondences [19]. The result of this step is a learning set of corresponding sample meshes.

4. Finally, based on the learning set of corresponding meshes from part three, a mean model and deformation modes can be extracted. The averaging can either be performed in the coordinate system of the landmark model or in a coordinate system resulting from a Procrustes analysis. According to our experience, the landmark based registration scheme works sufficiently well, a rigorous analysis of the influence of the registration scheme needs still to be performed.

The procedure described above is clearly biased by the selection of the root image. In order to reduce the influence, steps three and four may be iterated, similar to an iterative Procrustes procedures. The approximate time consumption of the above procedure is as follows. Step one requires about 5 min per structure. For all structures of the cardiac surface model this sums up to about one hour. The merging of structures in part two works largely automatically for nicely overlapping structures. Together with the remaining handcrafting step two requires again about one hour. The mesh adaptation to the set of learning samples in step three requires about 5 min. for the landmark definition and another 10 min. for the semi-automated adaptation procedure, summing up to 15 min. per learning sample. Thus, the construction of a model from 20 samples requires about 7 hours.

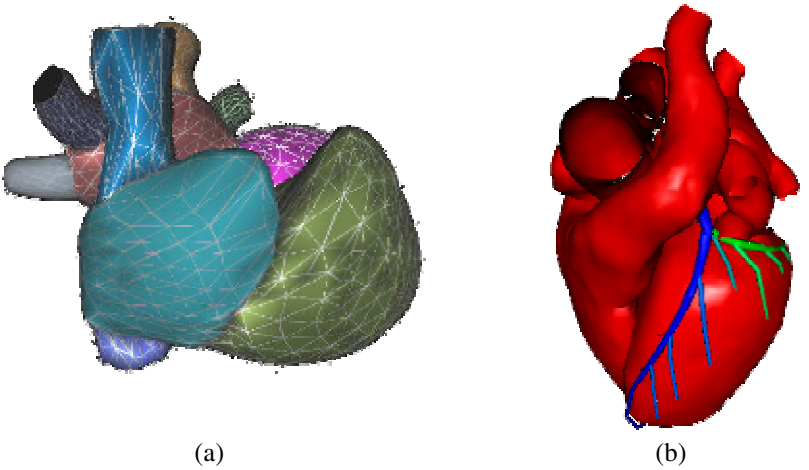

(a) (b)

Fig. 3. (a) Triangular meshes representing the cardiac surfaces. (b) Registered surface and coronary artery model

4.4 Adding Variability to the Model

As pointed out in section 2, we follow the idea of separating the representation of (mean) shape and the representation of deformation. The advantage of this approach is firstly that it intrinsically enables a coherent deformation of the model, independent of the representation and parameterization of the geometry of the model parts. Secondly, it allows using deformation fields that originate from other sources, e.g. from elastic registration procedures or from tagged or phase contrast MRI images. The approach is related to methods that use elastic registration during the model construction or adaptation phase [24-26]. In order to realize this approach we need a common scheme to represent deformation. The steps to achieve this are sketched as follows. We assume that a deformation measurement consists of a set of deformation

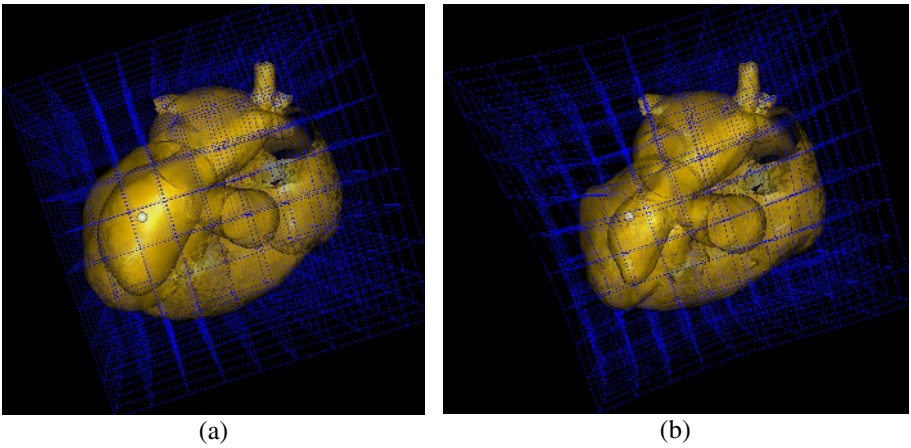

(a) (b)

Fig. 4. Result of the adaptation of the cardiac surface model to a multi-phase CTA dataset. (a) depicts the end-diastolic and (b) the end-systolic heart phase. Based on the motion of the mesh vertices a full-space deformation field as been interpolated using a thin-plate-spline approach, depicted by the blue grid-lines

vectors in a given coordinate system. This could be a set of corresponding vertices of a surface mesh propagated through a time series of images, or corresponding tag-line crossings of a tagged MRI image series, or the motion of a grid of control points derived from an elastic registration. In a first step the deformation vectors are transformed into the model coordinate system based on the registration of a sub-set of geometrical model-items that can be delineated in the source images (e.g. a set of cardiac landmarks). In the second step a smooth deformation field is interpolated from the (potentially sparse) input vectors, e.g. by a thin-plate-spline (TPS) interpolation approach [27], resulting in a smooth full space deformation field. In a third step, the deformation field now defined everywhere is sampled in a standardized way, e.g. on a Cartesian grid. Based on the representation resulting from step three, the deformation fields can be averaged or further statistically analyzed. Figure 4 shows a deformation

derived from surface tracking through the cardiac cycle. The end-diastolic (4a) and end-systolic (4b) shape of the cardiac surface model as adapted to a multi-phase cardiac CTA image is shown. The blue grid-lines visible in the images indicate the spatial deformation as derived from a TPS interpolation.

5 Conclusions and Future Work

The generation of a comprehensive geometrical model of the human heart has been described. Currently available is a mean model of the cardiac structures comprising the surfaces of the cardiac chambers and trunks of the connected vasculature, the coronary arteries and a set of 25 landmarks. The model is based on published data on the coronary arteries and on 20 multi-slice CT datasets. We advocate a distinct representation of the mean model geometry and model variability. A scheme to represent and add inter-individual and temporal variability to the model has been proposed. Current activities focus on enlarging the set of learning samples and on motion field extraction based on multi-phase cardiac CT and cine cardiac MRI image data. The next step will be the model application in the context of automated detection, segmentation and tracking of cardiac structures.

Acknowledgements

We would like to thank our colleagues from PMS-CT Cleveland, PMS-CT Haifa, PMS-MIT Best, PMS-MR Best, and PMS-XRD Best for the abundance of cardiac image material and many fruitful discussions. We also would like to thank J. T. Dodge for kindly making available updated position measurements of the coronary arteries.

References

1. A. F. Frangi, W. J. Niessen, and M. A. Viergever, "Three-Dimensional Modeling for Functional Analysis of Cardiac Images: A Review", IEEE Trans Med Imaging, vol. 20, no. 1, pp.2-25, Jan. 2001.
2. I. Haber, D. N. Metaxas, and L. Axel, "Three-dimensional motion reconstruction and analysis of the right ventricle using tagged MIR, Medical ImageAnalysis, vol.4, pp. 335-355, 2000.
3. A. F. Frangi, D. Rueckert, J. A. Schnabel, and W. J. Niessen, "Automatic Construction of Multiple-Object Three-Dimensional Statistical Shape Models: Application to Cardiac Modeling", IEEE Trans Med Imaging, vol. 21, no. 9, pp.1151-1166, Sep. 2002.
4. K. Park, D. N. Metaxas, and L. Axel, "LV-RV Shape Modeling Based on a Blended Parameterized Model", MICCAI 2002, LNCS 2488, pp. 753-761, 2002.
5. S. C. Mitchell, B. P. F. Lelieveldt, R. J. van der Geest, H. G. Bosch, J. H. C. Reiber and M. Sonka, "Multistage Hybrid Active Appearance Model Matching: Segmentation of the Left and Right Ventricles in Cardiac MR Images, IEEE TMI, vol. 20, no. 5, May 2001.

6. M. Lorenzo-Valdés, G. I. Sanchez-Ortiz, R. Mohiaddin, and D. Rueckert, "Atlas-Based Segmentation and Tracking of 3D Cardiac MR Images Using Non-rigid Registration", MICCAI 2002, LNCS 2488, pp. 642-650, 2002.
7. M. Lorenzo-Valdés, G. I. Sanchez-Ortiz, R. Mohiaddin, and D. Rueckert, "Segmentation fo 4D Cardiac MR Images Using a Probabilistic Atlas and the EM Algorithm", MICCAI 2003, LNCS 2878, pp. 440-450, 2003.
8. R. F. Schulte, G. B. Sands, F. B. Sachse, O. Dössel, and A. J. Pullan, "Creation of a human heart model and its customisation using ultrasound images", Biomedizinische Technik vol. 46, no. 2, 2001.
9. W. P. Segars, D. S. Lalush, and B. M. W. Tsui, "A Realistic Spline-Based Dynamic Heart Phantom", IEEE Trans nuclear science, vol. 46, no. 3, pp.503-506, June 1999.
10. N. P. Smith, A. J. Pullan, and P. J. Hunter, " Generation of an anatomically based geometric coronary model", Ann Biomed Eng. vol. 28, no. 1, pp. 14-25, 2000.
11. D. Sherknies, and J. Meunier, "A numerical 3D coronary tree model", Proc. 16th int. Congress and Exhibition Computer Assisted Radiology and Surgery (CARS'02), Springer, pp. 814-818, 2002.
12. C. Lorenz, J. von Berg, T. Bülow, S. Renisch, S. Wergandt, "Modeling the coronary artery tree", Shape Modeling Applications, 2004. Proceedings, pp. 354- 399, 2004.
13. J.T. Dodge, B.G. Brown, E.L. Bolson, and H.T. Dodge, "Intrathoracic spatial location of specified coronary segments on the normal human heart. Applications in quantitative arteriography, assessment of regional risk and contraction, and anatomic display", Circulation 78, pp. 1167-1180, 1988.
14. J.T. Dodge, B.G. Brown, E.L. Bolson, and H.T. Dodge, "Lumen diameter of normal human coronary arteries. Influence of age, sex, anatomic variation, and left ventricular hypertrophy or dilation", Circulation 86. pp. 232-246, 1992.
15. I. L. Dryden and K. V. Mardia, "Statistical Shape Analysis", Wiley, Chichester, 1998.
16. P.J. Scanlon, D.P. Faxon, "ACC/AHA Guidelines for Coronary Angiography", Journal of the American College of Cardiology, vol. 33, no. 6, pp. 1756-1824, 1999.
17. J. Lötjönen, S. Kivistö, J. Koikkalainen, D. Smutek, and K. Lauerma, "Statistical shape model of atria, ventricles and epicardium from short- and long-axis MR images", Medical Image Analysis, vol. 8, no. 3, pp. 371-386, Sep. 2004.
18. R. Pilgram, K. D. Fritscher, R. Schubert, "Modeling of the geometric variation and analysis of the right atrium and right ventricle motion of the human heart using PCA", Proc. 18th int. Congress and Exhibition Computer Assisted Radiology and Surgery (CARS'04), Springer, pp. 1108-1113, 2004.
19. M. R. Kaus, V. Pekar, C. Lorenz, R. Truyen, S. Lobregt, and J. Weese, "Automated 3-D PDM construction from segmented images using deformable models", IEEE TMI, vol. 22, no. 8, pp. 1005-13, Aug. 2003.
20. H. Timinger, V. Pekar, J. von Berg, K. Dietmayer, and M. Kaus, "Integration of Interactive Corrections to Model-Based Segmentation Algorithms", Bildverarbeitung für die Medizin Algorithmen, Systeme, Anwendungen. Proceedings des Workshops vom 9. - 11. März 2003 in Erlangen, Springer, 2003.
21. M.R. Kaus, J. von Berg, J. Weese, W. Niessen, and V. Pekar, "Automated segmentation of the left ventricle in cardiac MRI", Medical Image Analysis, vol. 8, no. 3, pp. 245-254, Sep. 2004.
22. J. von Berg, C. Lorenz, "Multi-Surface Cardiac Modeling, Segmentation, and Tracking", Functional Imaging and Modeling of the Heart, 2005. submitted
23. B. K. P. Horn, "Closed-form solution of absolute orientation using unit quaterions", Journal of the optical society of America A, Vol. 4, no. 4, pp. 629-642, 1987.

24. J. Lötjönen, D. Smutek, S. Kivistö, K. Lauerma, "Tracking Atria and Ventricles Simultaneously from Cardiac Short- and Long-Axis MR Images, MICCAI 2003, LNCS 2878, pp. 467-474, 2003.
25. M. Wierzbicki, M. Drangova, G. Guiraudon, ajnd T. Peters, "Validation of dynamic heart models obtained using non-linear registration for virtual reality training, planning, and guidance of minimally invasive cardiac surgeries, Medical Image Analysis, vol. 8, pp. 387-401, 2004.
26. A. Rao, G. I. Sanchez-Ortiz, R. Chandrashekara, M. Lorenzo-Valdés, R. Mohiaddin, and D. Rueckert, "Comparison of Cardiac Motion Across Subjects Using Non-rigid Registration, MICCAI 2002, LNCS 2488, pp. 722-729, 2002.
27. F. L. Bookstein, "Principal Warps: Thin-Plate Splines and the Decomposition of Deformations", IEEE PAMI, vol. 11, no. 6, pp. 567-585, 1989.